

ROLE OF INTERVENING Mg II ABSORBERS ON THE ROTATION MEASURE AND FRACTIONAL POLARISATION OF THE BACKGROUND QUASARS

SUNIL MALIK¹, HUM CHAND², T. R. SESHADRI¹

¹ Department of Physics and Astrophysics, University of Delhi, Delhi 110007, India

² Aryabhata Research Institute of Observational Sciences (ARIES), Manora Peak, Nainital– 263002, India
sunilmalik1993@gmail.com

ABSTRACT

Excess extragalactic contribution to residual rotation measure (RRM) for quasars sightlines with intervening Mg II absorbers is a powerful tool to investigate the presence of magneto-active plasma in high-redshift galaxies. To carry out such an analysis, we have compiled a large sample of 1132 quasars for which we have RRM data as well as optical spectra capable of ascertaining the presence/absence of any intervening Mg II absorbers. In this study, we found that the dispersion in RRM (σ_{rrm}) for 314 sightlines having Mg II intervening absorbers is 15.78 ± 0.92 rad m⁻² as compared to its value of 14.62 ± 0.70 rad m⁻² for the 818 sightlines without such absorbers, resulting in an excess standard deviation (σ_{rrm}^{ex}) of 5.93 ± 2.99 rad m⁻² among these two subsamples. A similar analysis on subsample split based on the radio spectral index ($F \propto \nu^\alpha$) for flat ($\alpha \geq -0.3$; 312 sources) and steep ($\alpha \leq -0.7$; 469 sources) show non-significant dependence of spectral index on σ_{rrm}^{ex} . An anti-correlation is found between the dispersion in RRM and fractional polarisation (p) with Pearson correlation coefficient (ρ_p) of -0.70 and -0.87 for the subsample with and without Mg II absorbers, respectively. This nominal impact of Mg II absorbers on ρ_p suggests that the main contribution for the decrement in the p value is intrinsic to the local environment of the quasars. Based on our subsample of quasars without Mg II absorbers, we found that neither σ_{rrm} nor the median value of the p , indicates any evolution with quasars emission redshift. However, a very significant correlation with $\rho_p = 0.85$ is found among σ_{rrm} and the Mg II absorber redshift. This can be useful to place strong constraint on models of magnetic field evolution in the high-redshift galaxies.

Subject headings: galaxies: luminosity, redshifts, magnetic fields – polarization, Stokes parameters, quasars: absorption lines, objects: quasars general – intergalactic medium – techniques: spectroscopic

1. INTRODUCTION

Magnetic field has a significant impact on several astrophysical processes such as transport and confinement of cosmic rays, star formation in the galaxy, cloud collapse, and galactic outflows (e.g., Mestel & Paris 1984; Rees 1987; Watson & Perry 1991; Vacca et al. 2018). To gauge the effect that magnetic field could have on these processes, we need to study the strength and morphology of the magnetic fields at different scales.

Several probes, such as, synchrotron radiation, Faraday rotation, Zeeman splitting, dust polarisation and dust emission, are available for this investigation. Among them, Faraday rotation (FR) is a powerful probe to study the strength of the line-of-sight component of the magnetic field over cosmic distances. The contribution to FR comes from the integrated value of the line-of-sight magnetic field along the path of sightline, weighted by the electron number density (e.g., Kronberg & Simard-Normandin 1976; Kronberg et al. 1977; Kronberg & Perry 1982; Welter et al. 1984; You et al. 2003; Kronberg et al. 2008; Bernet et al. 2008, 2010, 2012; Hammond et al. 2012; Bhat & Subramanian 2013). FR is quantified by the observed rotation measure (RM) which is defined as the difference in angle $\Delta\chi_0$ through which the plane of polarisation of radiation is rotated per unit interval of the square of the observed wavelength, $[RM = \Delta\chi_0/\Delta\lambda_0^2]$. For a linearly polarised radiation from a radio source at emission redshift, z_{emi} , $RM(z_{emi})$ is given by, (e.g. see

Bernet et al. 2012),

$$RM(z_{emi}) = \frac{\Delta\chi_0}{\Delta\lambda_0^2} = 8.1 \times 10^5 \int_{z_{emi}}^0 \frac{n_e(z) B_{\parallel}(z) dl}{(1+z)^2 dz}. \quad (1)$$

Here, RM is measured in units of rad m⁻², n_e is the number density of electron (n_e in cm⁻³), the longitudinal magnetic field component (B_{\parallel} in Gauss) and dl/dz is the column length (in parsecs) per unit redshift interval.

The individual contribution to RM can be expressed as a sum of the following four components:

$$RM = RM_{QSO} + RM_{IGM} + RM_{INT} + GRM, \quad (2)$$

where, RM_{QSO} is the intrinsic contribution coming from the source (i.e., the quasar) itself, RM_{INT} is the contribution coming from any intervening galaxies if they happen to be along the line of sight and GRM is the Galactic rotation measure of the Milky Way. The RM_{IGM} is the contribution of the intergalactic medium (IGM) which is likely to be negligible as compared to that of the other three source(s). The GRM contamination need to be removed so as to get the extra-galactic contribution, leading to the residual rotation measure (RRM) given by,

$$RRM = RM - GRM \quad (3)$$

One of the ways to measure GRM is by studying the

nature of polarisation of the signal from pulsars. Such rotation measures in our galaxy not only enables one to understand the various structures in the rotation measure sky (Roy et al. 2008; Schnitzeler 2010; Stil et al. 2011) but also can be used to estimate the GRM in different directions for our galaxy using smoothing functions (Han et al. 2006; Short et al. 2007; Xu & Han 2014a). Further, one can divide RRM sample into two subsamples, one consisting of $RM_{QSO} + RM_{IGM}$ for which the light does not pass through intervening galaxies and the other for which one or more galaxies fall in the line of light (i.e. $RM_{QSO} + RM_{IGM} + RM_{INT}$). The statistical properties of RRM in these two sub-samples, and more importantly the difference among them, can be a unique tool to probe the global properties of the magnetic fields at high redshifts (e.g., see below).

The RRM properties of the polarised quasar subsample whose light does not pass through intervening galaxies will be crucial to understanding the redshift evolution of cosmic magnetic field (Kronberg et al. 2008; Bernet et al. 2012; Hammond et al. 2012; Basu et al. 2018), while its difference as compared to the subsample of quasars with sightline passing through the intervening galaxies will give important clue about the magnetic field and its evolution in the high-redshift galaxies. However, it may be noted that the detection of galaxies in emission at high redshift, especially, on the sight-line of background bright quasars is difficult. On the other hand, these galaxies could easily be detected in the absorption of the many resonant atomic transitions such as Mg II, C IV doublets, in the spectra of background quasars, which is also free from any detection bias of galaxy based on their brightness. This implies that to classify the polarised quasar sight-lines with and without intervening galaxies we can use the presence/absence of such intervening absorption line systems in these quasar spectra.

Among the population of intervening galaxies along quasar sight-lines the best-studied are the ones selected using Mg II absorption lines. It is now well established that for Mg II systems with rest frame equivalent width $EW_r > 1.0 \text{ \AA}$, a galaxy is almost always found within an impact parameter of $\sim 100 \text{ kpc}$ (e.g., Steidel 1995; Churchill et al. 2005; Zibetti et al. 2007; Chen & Tinker 2008; Kacprzak et al. 2008) and spanning a wide range in optical luminosity (e.g., Bergeron & Stasińska 1986; Steidel 1995; Kacprzak et al. 2008). On the other hand, Mg II systems with $0.3 \text{ \AA} < EW_r < 1.0 \text{ \AA}$ are thought to predominantly trace separate populations of galaxies, such as low surface brightness galaxies, or dwarf galaxies or are absorber at high impact parameter (e.g., see Churchill et al. 2005; Narayanan et al. 2007). Therefore many past studies have used Mg II absorption systems to classify the sample of polarised background quasars with and without intervening galaxy contribution to RRM. As a result it can be a useful tool in the study of the magnetic field and its evolution in the high-redshift galaxies (e.g., Oren & Wolfe 1995; Kronberg et al. 2008; Bernet et al. 2008, 2010, 2012; Hammond et al. 2012; Bernet et al. 2013; Bhat & Subramanian 2013; Joshi & Chand 2013; Farnes et al. 2014b; Mao et al. 2017; Basu et al. 2018).

Bernet et al. (2008) used high-resolution spectra of 76 quasars and showed that quasars with stronger Mg II sys-

tems are associated with the larger RRM values at a wavelength of 6 cm. Subsequently, Bernet et al. (2010) showed that such an association of larger RRM exists only for Mg II absorbers having $EW_r > 0.3 \text{ \AA}$, and was absent for absorber with $EW_r \leq 0.3 \text{ \AA}$. This was further supported by the investigation of Bernet et al. (2013) where they found that sightline with Mg II systems having impact parameter $< 50 \text{ kpc}$ indeed have higher RM as compared to those with Mg II absorbers at higher impact parameter. Another technique to measure RRM based on the radio-synthesis method has been used by Kim et al. (2016). They confirm that intervening systems are strongly associated with depolarization and characterize the complexity of the Faraday Depth spectrum using a number of parameters including intrinsic depolarization in the background sources.

Similarly, statistical properties such as dispersion in RRM at different redshift bins have been used to infer the redshift evolution of cosmic magnetic field (e.g., see Welter et al. 1984; Watson & Perry 1991; Kronberg et al. 2008; Bernet et al. 2012; Hammond et al. 2012; Neronov et al. 2013). For instance, Kronberg et al. (2008) uses 268 sightlines with RM measurement at a wavelength of $\sim 10 \text{ cm}$ in their analysis and found that the distribution of RMs broadened with redshifts. However, Hammond et al. (2012), did not find any redshift evolution in the width of RMs distribution, where they have used a larger sample of 3650 quasars with rotation measure compiled using a catalog of Taylor et al. (2009), based on NRAO VLA SKY SURVEY (NVSS) at wavelength of 21 cm. This lack of firmness could be due to the fact that the sample used in this study is a mixture of sightlines with and without intervening absorbers. Since different intervening absorbers can have different absorption redshift, they may alter their analysis of RRM pattern being probed at various emission redshift bins of the background polarised quasars.

In an attempt to understand this discrepancy, Bernet et al. (2012) also analyzed the dataset of Taylor et al. (2009) based on NVSS radio data at 21 cm, where they had separated the sightlines with and without intervening absorbers. They compared their results with the work of Kronberg et al. (2008) and Hammond et al. (2012) who too used the RM values at a wavelength of 21 cm, and with the Bernet et al. (2008, 2010) who used RM values at a wavelength of 6 cm. They too did not find either an increase of the RM dispersion with redshift or any correlation of RM strength with Mg II absorption lines contrary to the result at 6 cm by Bernet et al. (2008, 2010). To reconcile this discrepancy, they have proposed an inhomogeneous Faraday screen model due to the intervening absorbers/galaxies which dilute the RRM contribution at 21 cm more as compare at the wavelength of 6 cm. Later, Joshi & Chand (2013) investigated the dependence of RRM at 21 cm on intervening absorption systems with an enlarged sample consisting of 539 quasars separated out in the subsample with and without Mg II absorbers. In their study, they found that dispersion in RRM (σ_{rrm}) at 21 cm and the presence of Mg II absorbers are correlated though only at about 1.7σ level, and hence at a lesser confidence level compared to the above studies at the wavelength of 6 cm (though using relatively smaller sample).

As an alternative route to understand the above discrepancy in the correlation of σ_{rrm} vis-a-vis Mg II absorbers presence at wavelength of 21 cm and 6 cm, [Farnes et al. \(2014b\)](#) explored the effect of apparent frequency-dependent observational selection bias. This could arise because one may select different source populations, with different morphology and position in relation to the optical counterparts at these high and low radio frequencies observations. They used the spectral index as a criterion to split their sample of 599 sources having optical spectra, RM and spectral slope, into flat-spectrum and steep-spectrum subsamples. In their analysis, they found that the flat-spectrum sample shows significant (at $\sim 3.5\sigma$ level) evidence of a correlation between the presence of Mg II absorption and dispersion in RM measurement at ~ 21 cm, while their steep-spectrum sample shows no such correlation.

Apart from the RRM measurement for these quasars sightlines, their observed fractional polarisation (p) is another parameter which might also be a useful tool to probe the magnetic field in the intervening galaxies, again by comparing p values and its correlation with RRM for subsample with and without Mg II absorbers. Many past studies have explored this possibility and found that indeed higher RRM is associated with the lesser p value ([Hammond et al. 2012](#); [Bernet et al. 2013](#); [Kim et al. 2016](#)). For instance, [Hammond et al. \(2012\)](#) found an anti-correlation between RRM and fractional polarization. One possible physical bias suggested by them was the presence of intervening absorbers, recalling the fact that RM distribution used in their study, have a mixture of sightlines with and without the Mg II absorbers.

It is evident from the above existing studies that while using the RM to understand the magnetic field of the high- z galaxies and their evolution, it is important to remove various degeneracies in the observed RM value caused by different contributions (e.g., see Eq. 2). This necessitates the splitting of the sample into various subsamples based on either the radio spectral slope and/or the presence/absence of the intervening absorbers. As pointed out above such splitting will also lead to small statistics problem which may not allow one to draw any firm conclusion on the nature of the magnetic field based on RM studies. It may be noted that the main hindrance in improving the sample size in such studies is the scarcity of the optical spectra for the sample having RM measurements, which is very crucial to separate out quasars sightline with and without the intervening galaxies reveal as the intervening Mg II absorbers.

However, with the advent of the large spectroscopic survey such as Sloan Digital Sky Survey (SDSS) Data Release(DR)-7, 9, 12 & 14, it has now become possible to enlarge the rotation measure sample for which optical spectra is available. Additionally, the catalogs of Mg II absorption lines for the SDSS spectra has been published by [Zhu & Ménard \(2013\)](#) using DR-7, 9 and by [Raghunathan et al. \(2016\)](#) using DR-12,14.

At the same time, large radio catalogs of RM such as compiled by [Taylor et al. \(2009\)](#) are now available. It consists of RM measurements of 37,453 sources (e.g., see Sect. 2 for more detail). One also has radio spectral slope compilation of [Farnes et al. \(2014a\)](#) consisting of 25,649 sources. It is useful to cross-correlate these opti-

cal catalogs with these large radio catalogs of RM. This forms the main motivation of our work in this paper in which we have doubled the sample size by including the above mentioned newer SDSS Data releases. We split the sample into subsamples based on either the radio spectral slope and/or the presence/absence of the intervening absorbers. Such enlarged sample will be very useful (i) to quantify the role of intervening galaxies and their equivalent widths on RRM by comparing subsamples with and without intervening absorbers, along with their subsamples such as steep and/or flat-spectrum radio quasars, (ii) probe any redshift evolution of RRM (by using a subsample without intervening absorber), and (iii) search for any effect of the intervening absorbers on the fractional polarization of the background quasars; so as to finally infer the presence and strength of magneto-active plasma in these high redshift galaxies.

The paper is organized as follows. We discuss the nature of our sample which we assembled from several optical and radio catalog in Sect. 2. Further, in Sect. 3 we discuss the classification of our sample into subsamples based on quasar sightlines, with and without intervening Mg II absorbers. In Sect. 4 we present our analysis and results, while in Sect. 5 we discuss our major findings and present our conclusions.

2. THE SAMPLE

Our study requires a sample of quasars, for which RM measurement as well as optical spectra are available. In this study, we have used archival data for RM as well as for optical spectra. For RM measurement of quasars, we identified two main catalogs in literature given by [Taylor et al. \(2009, henceforth TSS09\)](#)¹ and [Xu & Han \(2014b\)](#). In [Xu & Han \(2014b\)](#) they have compiled RM data for 4553 sources using observation in the frequency ranging from 1.3 GHz to 2.3 GHz. In addition to RM, they have also given the Galactic Rotation Measure (GRM) for each of the sources. On the other hand, the TSS09 catalog consisting of RM for 37,543 sources, is based on the NVSS observations, where they have used Q and U Stokes Parameters in two frequency bands, 1364.9 MHz and 1435.1 MHz to estimate the polarised intensity and polarisation fraction. The sample in [Xu & Han \(2014b\)](#) has been found very useful to get the GRM value for many of our sources (see below). However, to avoid the inhomogeneity due to the mixing of two catalog, we have only used TSS09 as our reference catalog for RM measurement. By not using the sample of [Xu & Han \(2014b\)](#), there has been only a nominal impact of just 2.7% reduction on our final sample size.

For searching the optical counterpart of the quasars with RM measurement in TSS09, we have used SDSS DR-7, 9, 12 & 14 catalogs of quasars for their optical spectra. The additional advantage of these optical surveys apart from being large and homogenous is that for them a systematic investigation has been carried out to search for the presence of Mg II intervening absorbers along the line of sight of their quasars. For DR-7, ² this compilation has been carried out by [Zhu & Ménard](#)

¹<http://www.ucalgary.ca/ras/rmcatalogue>

²<http://www.guangtunbenzhu.com/jhu-sdss-metal-absorber-catalog>

(2013, henceforth ZM13) and for SDSS DR-12, 14³ by Raghunathan et al. (2016, henceforth RS16).

Using these catalogs we have made our sample based on the following selection criteria;

(i) *Redshift range*: From the SDSS Mg II catalogs both by ZM13 and RS16, we have retained only those quasars whose emission redshift is in the range $0.38 \leq z_{emi} \leq 2.3$. The upper redshift cutoff of 2.3 is imposed based on the upper limit of 9000 Å on the wavelength of the SDSS spectrum. For quasars with redshift more than this limit, the Mg II emission lines is beyond the SDSS spectral coverage. Hence, our upper limit avoids the ambiguity of any Mg II absorber falling above the spectral coverage. Our lower limit of 0.38 on the emission redshift ensures that the starting observed wavelength of SDSS spectra at 3800 Å allows us to detect at least one Mg II doublet if present.

(ii) *Radio and optical position offset*: We cross-correlate the RM catalog of TSS09 with the total quasars searched for making the SDSS Mg II absorption line catalogs (i.e., ZM13 and RS16) fulfilling the above redshift criterion (i.e., $0.38 \leq z_{emi} \leq 2.3$), by demanding that their optical and radio position matches within an offset of less than 7 arcsec.

The details of the outcome of this cross-correlation among these catalogs are given in Table 1. Columns 1 & 2 give the names of SDSS optical catalog and the total number of quasars in them, while columns 3 and 4 give the number of quasars fulfilling the redshift constrain of $0.38 \leq z_{emi} \leq 2.3$ and the positional match with the TSS09 RM catalog within an offset of 7 arcsec. The 5th column gives the number of sources that are finally considered after discounting the repetition of sources which can happen due to repeated observation within various SDSS data releases. As can be seen from this table (last column) that after removal of the duplication among various data releases of SDSS for quasars, the SDSS DR-7, 9, 12 and 14 have contributed 673, 23, 257 and 182 quasars respectively, leading to the merged sample of 1135 sources. Further, we have noted that in the catalog of TSS09 based on NVSS the value of GRM is not available, hence, we have made use of the GRM compilation by Xu & Han (2014b). Out of our 1135 sources, 134 sources were common with Xu & Han (2014b) and hence we could use the GRM value for them from this catalog. For the remaining 1001 sources, we used the online GRM calculator⁴ of Xu & Han (2014b) to estimate the GRM value. Here, we have assumed that the error in GRM due to the difference in the measurement frequency (1.3 - 2.3 GHz in the Xu & Han (2014b) and 1.4 GHz in the TSS09) is negligible compared to typical uncertainty in the GRM measurement.

In the left panel of Fig. 1 we have plotted the distribution of RRM (i.e., RM-GRM) for our sample which is well fitted (using r.m.s minimization) by a Gaussian function with best fit 1σ width parameter of 14.99 rad m⁻².

In this distribution, we noted three outliers in RRM

with values of 142.4 (SDSS J012142+114950), -473.8 (SDSS J111857+123442) and -172.1 rad m⁻² (SDSS J110120+415308) which deviate from the mean at more than 9σ level. After excluding these three outliers, we are left with 1132 sources for our final analysis with typically 81.89%, 96.11%, and 99.55% fraction of our sources having $|RRM| \leq 25, 50$ and 100 rad m⁻², respectively. The right panel of Fig. 1 shows that the distribution for RM is also found to be well fitted with Gaussian function albeit with higher width and mean value as compared to the RRM distribution. The details about our final sample of 1132 source is given in Table 2. Column 1 gives the SDSS name (i.e., optical position) of our sources, while columns 2 to 7 give RM, GRM, RRM along with their errors. Column 8 gives the number of Mg II absorbers along the source sightline (n(Mg II)) while the 9th column gives the emission redshift. Columns 10 and 11 give the fractional polarisation and its error and the column 12 give radio spectral indices (using $F_\nu \propto \nu^\alpha$).

3. CLASSIFICATION OF SIGHTLINES BASED ON THE NUMBER OF Mg II ABSORBERS

As pointed out in the previous section, to classify the sightlines with and without intervening systems, we have utilized the catalogs of Mg II absorption systems given by ZM13 for the quasar's spectra of the SDSS DR-7 & 9. However, for the spectra taken from the SDSS DR-12 & 14 the Mg II catalog given by RS16 has been used. This has allowed us to split our sample into two subsamples viz., with (n(Mg II)>0) and without (n(Mg II)=0) intervening Mg II system, and hence to probe the correlation of the rotation measure with the presence of Mg II intervening absorbers (see below). These catalogs give information on Mg II absorption systems such as the number of Mg II absorbers, their absorption redshifts (z_{abs}) and equivalent widths (along with the associated error bars). Details about these catalogs are available in their parent catalog papers. In brief, both these catalogs have used a procedure based on an automated algorithm to search for Mg II absorption line features in the normalized quasar spectrum. The criterion for accepting a feature as genuinely arising from a Mg II absorption system is that at least two of the Mg II absorption lines, viz. Mg II $\lambda\lambda 2796, 2803$, are found at the expected doublet separation at the adopted detection threshold. Such a feature is further corroborated by the presence of the corresponding metal lines such as Fe II $\lambda 2600$.

Based on these catalogs, we used the outcome of their search for Mg II absorber systems to ascertain the presence of any intervening absorbers along the sightline of each quasar in our sample. We noticed that out of 1132 sightlines in our sample, 314 quasars sightlines have at least one Mg II absorber and remaining 818 quasar sightlines are without any such Mg II absorbers. Among the 314 sightlines, 237 quasars have one absorber each, 59 have two absorbers each and 18 have more than two absorbers, resulting in total detection of 409 Mg II absorption systems with their detailed properties as listed in Table 3. In this table, column 1 give the SDSS name (i.e., optical position) of our sources, whereas 2nd to 4th columns give z_{emi} , z_{abs} and error in z_{abs} , respectively. Columns 5 & 6 has the information about the rest frame equivalent width and its associated errors. This allowed us to make statistical sub-samples out of our full sam-

³<http://srini.ph.unimelb.edu.au/mgii.php>

⁴<http://zmtt.bao.ac.cn/RM/searchGRM.html>

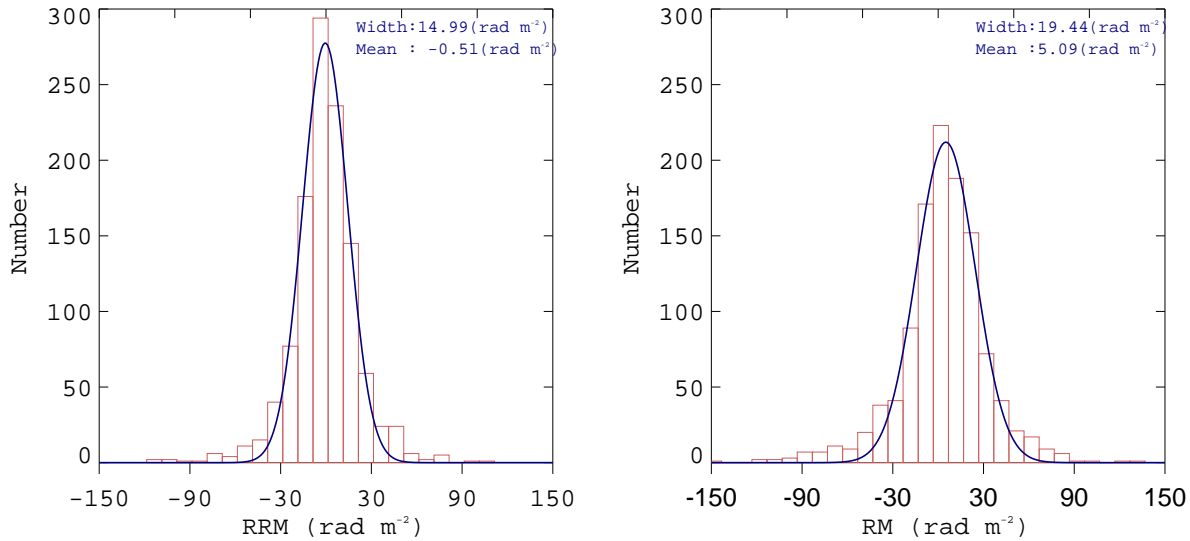


FIG. 1.— *Left panel:* Histogram of RRM (thin solid red line) for our 1132 sources, fitted (using r.m.s minimization) with the Gaussian function (thick solid blue line). *Right panel:* Same as left, but for the RM measurements. The impact of subtract the GRM is evident from the decrement of mean and standard deviation values of the RRM distribution as compared to the RM distribution.

TABLE 1
DETAILS ABOUT OUR SELECTION OF 1135 QUASARS SAMPLE.

Catalog name	Optical catalog of Mg II system		Cross-match with TSS09 RM catalog	
	Total quasars	quasars $0.38 \leq z_{emi} \leq 2.3$	Match found ^a	Taken ^b
SDSS DR-7 (ZM13) ^c	84533	26761	673	673
SDSS DR-9 (ZM13)	15439	7127	51	23
SDSS DR-12 (RS16) ^d	266403	37694	404	257
SDSS DR-14 ^e	525982	39969	588	182

^aNumber of sources found common within 7 arcsec between total quasars in redshift range of $0.38 \leq z_{emi} \leq 2.3$ in optical catalog and the TSS09 RM catalog. The TSS09 catalog has RM measurements of 37,543 sources at wavelength of 21 cm based on NVSS data.

^bThe different data release of SDSS also have repetition of spectral observations for many quasars, as a result, the number of sources taken for our sample can be smaller than the cross-match found (with 7 arcsec) between the optical and the radio catalog.

^cZhu & Ménard (2013) used for Mg II absorption line catalog of the SDSS DR-7, 9.

^dRaghunathan et al. (2016) used for Mg II absorption line catalog of the SDSS DR-12.

^eBased on publically available Mg II absorption line catalog of SDSS DR14 by Raghunathan et al. (2016) (e.g., see <http://srini.ph.unimelb.edu.au/mgii.php>).

TABLE 2
MAIN PROPERTIES OF OUR 1132 QUASARS SAMPLE (AFTER DISCOUNTING 3 OUTLIERS).

SDSS Name	RM	δRM	GRM	δGRM	RRM	δRRM	n(Mg II)	z_{emi}	p	δp	α
(1)	(2)	(3)	(4)	(5)	(6)	(7)	(8)	(9)	(10)	(11)	(12)
J142746+002848	25.30	13.60	3.90	6.10	21.40	14.91	0	1.26	5.97	0.37	...
J003936+204912	-23.30	6.50	-24.40	8.20	1.10	10.46	0	1.38	3.07	0.10	-0.77
J095443+403636	-3.10	3.80	-1.00	4.20	-2.10	5.66	1	0.78	5.53	0.10	-0.97
J083824+123000	30.80	9.40	29.80	7.30	1.00	11.90	2	1.62	3.75	0.17	-0.96
...

Note: The entire table is available in the online version. Only a portion of this table is shown here, to display its form and content.

ple of 1132 sources based on the number of intervening absorbers, being null, only one and at least one intervening absorbers as listed in Table 4 (see cols. 1, 2), for further analysis to find any correlation of RRM with the presence of intervening Mg II absorbers. The typical measured rest-frame equivalent width (e.g., see cols. 5,6 of Table 3) of the Mg II absorbers in our sample varies from 0.13 to 5.46 Å.

4. ANALYSIS AND RESULTS

4.1. Comparison of RRM distribution for subsample with and without Mg II absorbers

As pointed out in Sect. 1 the quasars with intervening absorption systems along their line of sight are expected to have broader RM distributions, due to extra scatter by the possible non-zero random component of

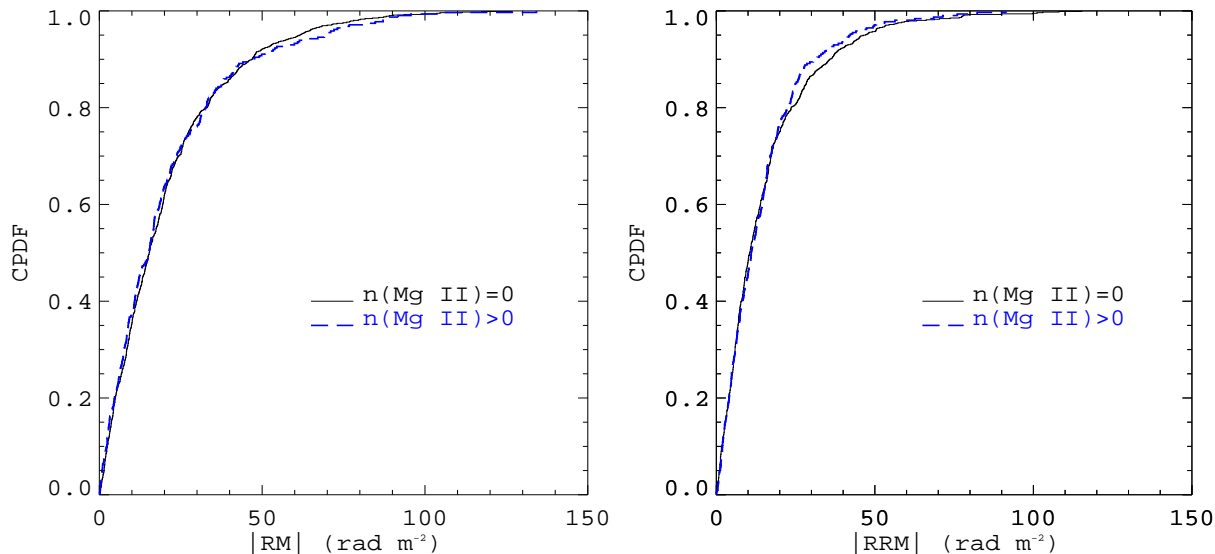


FIG. 2.— *Left panel:* Cumulative probability distribution (CPDF) of the absolute value of RM (i.e., $|RM|$), for the quasar with no absorber (black solid line), with absorbers (blue dashed line). *Right panel:* same as left, but for the $|RRM|$ measurements.

TABLE 3
MAIN PROPERTIES OF OUR 409 MG II ABSORPTION SYSTEMS SEEN TOWARDS 314 QUASARS SIGHTLINES IN OUR SAMPLE.

SDSS Name (1)	z_{emi} (2)	z_{abs} (3)	δz_{abs} (4)	$EW_r(\text{\AA})$ (5)	$\delta EW_r(\text{\AA})$ (6)
J095443+403645	0.78	0.74	0.72	0.90	0.09
J024534+010814	1.53	1.11	0.00	1.87	0.16
J003032-021156	1.80	1.37	0.00	1.83	0.06
J003032-021156	1.80	1.45	0.00	1.42	0.05
...
...

Note: The entire table is available in the online version. Only a portion of this table is shown here, to display its form and content.

the magnetic field of the galaxies associated with these absorbers, as compared to the sightlines without such intervening absorbers. To compare the RRM using with our enlarged sample of 1132 sightlines, in the left panel of Fig. 2 we have shown the cumulative probability distribution of the absolute value of RM ($|RM|$) for sightlines with and without Mg II absorbers. The K-S test rules out the null hypothesis (being drawn from the same distributions) at a confidence level of only $\sim 26\%$, which is not significant. However, it is also possible that the variation in GRM might also smear out the difference between these two subsets. To see such an effect of GRM we have also plotted the cumulative probability distribution of the absolute value of RRM ($|RRM|$) in the right panel of Fig. 2. The K-S test, now rules out the null hypothesis at a confidence level of $\sim 32\%$, which is also not significant.

To quantify the broadening of RRM distribution due to intervening absorbers, the commonly used method is to compute the dispersion of RRM for subsamples with and without Mg II absorbers. However, it may be noted that the dispersion of RRM around the mean can also be easily dominated by outliers (if any) in the distributions. An alternative approach to minimize any outlier effect is to use a distribution function for the RRM. As

shown in Fig. 3, this is well described by a Gaussian. The figure shows the Gaussian fit to the RRM distributions of sightlines without any absorber (top panel), with one absorber (middle panel), and for at least one absorbers (lower panel). The fit is carried out based on r.m.s minimization to derive the best fit values of the Gaussian parameters namely the mean, the width (σ_{rrm}) and the peak height of the Gaussian.

To estimate the typical error bar on these best-fit parameters we have adopted the Monte-Carlo simulation approach. Here, we assume the measured RRM values of individual quasars to be distributed as a Gaussian with mean value as our measured RRM value and width as our measured 1σ uncertainty. Based on this distribution we have drawn random 1000 values corresponding to each measured RRM value, leading to 1000 realizations of RRM sample to estimate the distribution of their best-fit parameters. The distribution of the best-fit width's of these 1000 realizations of RRM is also well distributed as a Gaussian whose standard deviation we have assigned as uncertainty in our best fit σ_{rrm} listed in Fig. 3 and Table 4. Throughout the analysis, the error on the best fit is determined by using a similar Monte-Carlo simulation technique unless specified otherwise.

As can be noted from the plots shown in Fig. 3, the RRM distribution for the sightlines that pass through the Mg II absorbers is broader than the sightlines with no such intervening absorbers. The best fit σ_{rrm} for subsample with (i.e., $n(\text{Mg II}) > 0$) and without (i.e., $n(\text{Mg II}) = 0$) intervening absorbers is found to be $15.78 \pm 0.92 \text{ rad m}^{-2}$ and $14.62 \pm 0.70 \text{ rad m}^{-2}$, respectively. It can also be noticed that the subset with one Mg II absorber (i.e., $n(\text{Mg II}) = 1$) has also larger σ_{rrm} of $14.91 \pm 1.10 \text{ rad m}^{-2}$ than the subset without such intervening absorbers.

To quantify the excess broadening (σ_{rrm}^{ex}) found along the sightlines with intervening absorbers, we have subtracted the σ_{rrm} for the quasar subset with ($\sigma_{rrm(w)}$)

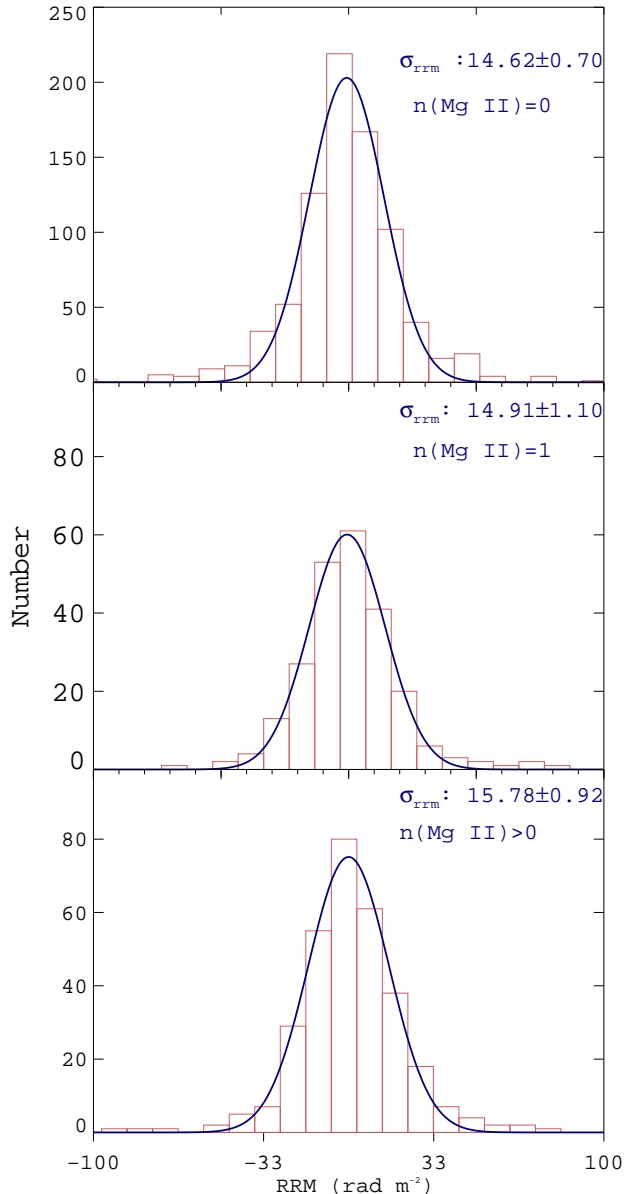


FIG. 3.— Histogram of RRM with no absorber ($n(\text{Mg II}) = 0$, upper panel), with one absorber ($n(\text{Mg II}) = 1$, middle panel) and with at least one absorbers ($n(\text{Mg II}) > 0$, lower panel), along with their fit using a Gaussian function. The fit is done using r.m.s minimization and the error bar on fitted Gaussian width (σ_{rrm}) is obtained by carrying Monte-Carlo simulation using the error on RRM (e.g., see Sect. 4.1).

and without ($\sigma_{rrm(w_0)}$) Mg II absorber in quadrature as,

$$\sigma_{rrm}^{ex} = \sqrt{\sigma_{rrm(w)}^2 - \sigma_{rrm(w_0)}^2}. \quad (4)$$

The excess in the standard deviation is found to be $5.93 \pm 2.99 \text{ rad m}^{-2}$, where the associated error is computed with error propagation as,

$$\delta\sigma_{rrm}^{ex} = \frac{1}{\sigma_{rrm}^{ex}} \sqrt{\sigma_{rrm(w)}^2 \delta\sigma_{rrm(w)}^2 + \sigma_{rrm(w_0)}^2 \delta\sigma_{rrm(w_0)}^2}. \quad (5)$$

This suggests that the intervening absorbers do contribute to RRM (though with nominal significance level)

and hence gives an indirect proof of the presence of the magnetic field in the disks/halos of these high redshift galaxies which are associated with these Mg II absorbers (e.g., see also Kronberg et al. 2008; Bernet et al. 2010; Joshi & Chand 2013).

Additionally Bernet et al. (2010) though with relatively smaller sample of 77 sources have also investigated the impact of the strength of absorption systems on the measured RRM, where they found that systems with equivalent width, $EW_r < 0.3 \text{ \AA}$ do not contribute significantly to the RRM (see also Bernet et al. 2013; Farnes et al. 2014b). It is expected that larger EW_r is more likely to arise for sightlines with small impact parameter to the intervening galaxy. Therefore to check such an effect of impact parameter on RRM we have studied its variation at different EW_r bin, the results of which are plotted in Fig 4.

Furthermore, if these intervening systems have a relatively stronger magnetic field, the observed scatter in RRM values will also be more. Therefore, to check for such an effect, we first computed σ_{rrm} for the subsample having EW_r smaller and larger than the median EW_r of 0.93 \AA in our sample. We found the σ_{rrm} to be $14.50 \pm 1.34 \text{ rad m}^{-2}$ and $15.15 \pm 1.79 \text{ rad m}^{-2}$ for subsamples of $EW_r \leq 0.93 \text{ \AA}$ and $EW_r > 0.93 \text{ \AA}$, respectively, based on their Gaussian fit (as shown in Fig. 4). Though the higher EW_r subsample show higher σ_{rrm} value but the difference in the dispersion is not significant with an excess of $4.93 \pm 7.59 \text{ rad m}^{-2}$.

Similarly, we also plotted the RRM and dispersion of RRM at different EW_r bin as shown in the right upper and lower panel of Fig. 4 respectively. Here too there is an indication of a tentative trend of increasing σ_{rrm} with higher EW_r bin though have a low significance level due to low statistics in each bin.

4.2. Intervening Mg II absorbers correlation with rotation measure for flat and steep spectrum sources

As pointed out in Sect. 4.1, our sample of 1132 sources do show a nominal correlation, between the presence of the intervening Mg II absorber and higher dispersion of RRM measured at 1.4GHz. It may further be noted that our sample may also consist of sources with compact morphology as well as sources dominated by extended lobes. This could lead to the physical situation where optical and radio sightlines are more likely aligned in compact sources (i.e., flat spectrum) while misalignment can happen in extended sources (i.e., steep spectrum) as proposed first by Farnes et al. (2014b). As a result, for the sightlines pointing towards the lobes dominated radio sources, there are chances that intervening absorbers which are being identified by optical spectra, might not be intercepting the radio flux. Hence their effective contribution in enhancing the dispersion of RRM might be lower as compared to the sightline pointing towards the core dominated radio sources (being more aligned with the optical sightline). Indeed, Farnes et al. (2014b), have used these aspects to quantify the correlation of the presence of intervening Mg II absorbers with that of Faraday rotation by analyzing two subsample based on their radio spectral index, α , ($F \propto \nu^\alpha$): one with lobe dominated extended radio sources represented by steep

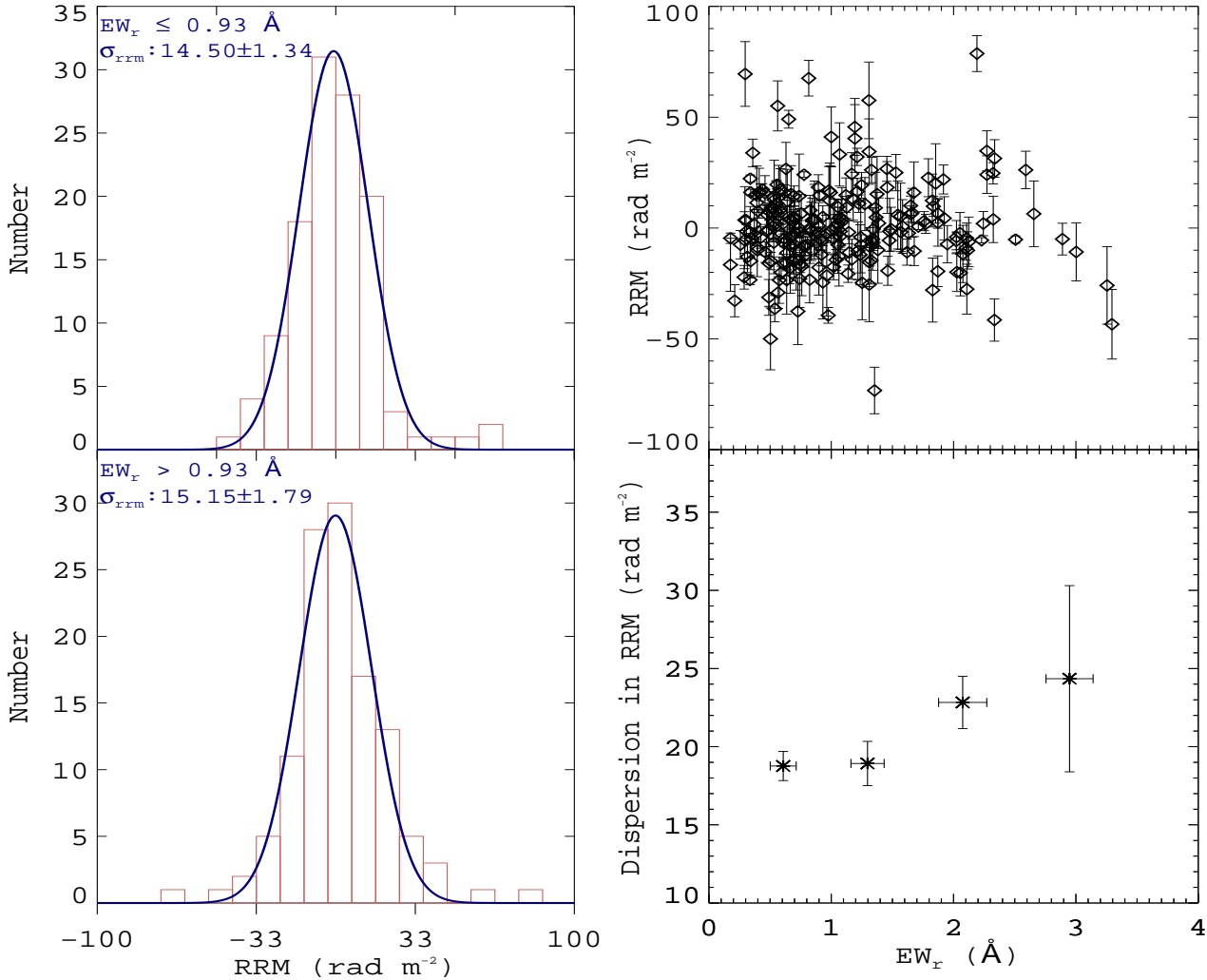


FIG. 4.— *Left panel:* Histogram of RRM with rest-frame equivalent width, EW_r , smaller (upper) and larger (lower) than the median of EW_r of 0.93 Å of our sample. *Right panel:* The plot of RRM with 1σ error bar (upper panel) and RRM r.m.s standard deviation in different EW_r bin (lower panel), based on 237 quasars with only one Mg II absorber. Here the error bar on r.m.s scatter is computed by propagating the individual error bar on RRM.

TABLE 4
RESULTS OF RRM DISTRIBUTION FOR VARIOUS SUBSAMPLE.

Sample type	Number of sources ^a	$\sigma_{rrm} \pm \delta\sigma_{rrm}$	$\sigma_{rrm}^{ex} \pm \delta\sigma_{rrm}^{ex}$ ^b	$P_{null}(\%)$ for RRM ^c
n(Mg II) = 0	818	14.62 ± 0.70
n(Mg II) = 1	237	14.91 ± 1.10	2.93 ± 6.60	79.65
n(Mg II) > 0	314	15.78 ± 0.92	5.93 ± 2.99	69.45

^aHere we have listed the total number of sources in each subset used in our analysis.

^bThe excess in σ_{rrm} in each subsample with respect to the n(Mg II) = 0 subsample.

^cThe percentage probability of null hypothesis using K-S test for a subsample with respect to n(Mg II) = 0 subsample.

spectrum with $\alpha \leq -0.7$ and another with core dominated compact radio sources having flat spectrum with $\alpha \geq -0.3$. Their sample consist of total 599 sources, among them, 142 and 232 belong to the flat and steep spectrum category respectively. In their study, they found a significant (at $\approx 3.5\sigma$ level) correlation between the Mg II absorbers and RM in the subsample of flat spectrum (core dominated) sources while it was absent in the subsample of steep spectrum (lobes dominated) sources. We have also carried out an analysis similar to that in

et al. (2014b) by making use of our bigger sample of 1132 sources for which we have both RM/RRM measurement as well as information about the presence/absence of any Mg II systems in their sightlines. For the values of spectral indices, we make use of its compilation by Farnes et al. (2014a), where they have compiled values of α for 25649 sources. After cross-correlating our sample of 1135 sources with Farnes et al. (2014a), we could get the α values for 1082 sources. Among them 469 have $\alpha \leq -0.7$ and 312 with $\alpha \geq -0.3$ as summarised in Table 5. It

may be noted that our sample provides almost a factor of two improvements in the sample size as compared to the [Farnes et al. \(2014b\)](#) sample, with the addition of 483 new sources.

Based on the above enlarged sample of 1082 sources that we consider, we searched for any difference in the correlation between the presence of Mg II and broadening in RRM distribution based on samples of flat and steep spectrum radio sources. As shown in the top two panels of [Fig. 5](#), we found that for a sample of flat-spectrum sources the dispersion of RRM value for subsamples with and without Mg II absorbers sightlines is found to be $15.76 \pm 1.97 \text{ rad m}^{-2}$ and $13.81 \pm 1.37 \text{ rad m}^{-2}$ respectively with an excess of $7.59 \pm 4.74 \text{ rad m}^{-2}$. In [Fig. 6](#) we have also plotted the cumulative probability distribution of the RRM for subsample without and with Mg II absorbers for flat spectrum sources as well as for steep spectrum sources. The KS-test for flat spectrum sources rule out the null hypothesis at $\sim 85\%$ confidence level (i.e. $P_{null} \sim 15\%$) that the RRM values of the subsamples (with and without Mg II absorbers) being drawn from the same distribution. On the other hand, for steep spectrum sources it is ruled out at a much lower confidence level of just $\sim 48\%$ only (i.e. $P_{null} \sim 52\%$). On the other hand, the lower two panels of [Fig. 5](#) show that for the steep spectrum sources, the dispersion of RRM for subsample with and without Mg II absorbers is found to be $16.37 \pm 1.69 \text{ rad m}^{-2}$ and $14.65 \pm 1.15 \text{ rad m}^{-2}$ respectively, with an excess of $7.70 \pm 4.44 \text{ rad m}^{-2}$. It may be noted that although the above corrections are not very significant, being at 85% confidence level in flat-spectrum sources in contrast to just $\sim 48\%$ for the steep spectrum sources, but a tentative trend seems to exist but not at high significance level (e.g., at 3.5σ) as reported by [Farnes et al. \(2014b\)](#).

Furthermore, it may be noted that in [Farnes et al. \(2014b\)](#) they have used RM in their analysis, however in our analysis, we have used RRM (i.e., the Galactic contribution is subtracted out). To check for any possible role of the Galactic rotation measure in the above discrepancy of the significance level, we also repeated our analysis using the 462 sources which are found common with the [Farnes et al. \(2014b\)](#) sample of 599 sources. Repeating the above analysis by splitting these 462 sources in subsample of $\alpha \leq -0.7$ (186 sources) and ≥ -0.3 (128 sources), we found that the correlation between the presence of Mg II absorber and dispersion in RRM is significant in the flat spectrum sources, but almost absent in steep spectrum sources. This suggests that the result of [Farnes et al. \(2014b\)](#) may not be affected by any bias due to the absence of correction for Galactic contribution at least based on these 462 sources. Although our sample size was a factor of two larger than theirs, we could not reproduce the high significance difference that they have found at 3.5σ level.

4.3. Correlation of RRM with fractional polarization

As pointed out in [Sect. 1](#), [Hammond et al. \(2012\)](#) have used a large sample of 3650 quasars in their analysis of RRM and fractional polarization along with their redshift evolution. Their analysis hints at an anti-correlation of RRM with fractional polarization. As we noted, their sample was a mixture of sightlines with and without intervening absorbers. One source of physical

bias proposed by them was the possibility of intervening absorbers increasing the scatter in RRM and decreasing the fractional polarization. Furthermore, [Bernet et al. \(2013\)](#) and [Kim et al. \(2016\)](#) also study the effect of intervening absorbers on the fractional polarization. [Bernet et al. \(2013\)](#) have found a correlation between the ratio of fractional polarization at wavelengths of 21 cm to that at 1.5 cm with the impact parameters of sightlines with the intervening galaxies. The possible mechanism for such depolarization could be such as differential Faraday rotation and/or due to the beam depolarisation (e.g., see [Kim et al. 2016](#)).

To test such a hypothesis using our sample, we first plotted the RRM versus p in the upper panel of [Fig. 7](#) based on the available p value for all the 1132 sources in our sample. To quantify the trend of decrease in scatter with the increase in p as evident in this figure, we have also plotted the dispersion of RRM in various bins of p as shown in the lower panel of [Fig. 7](#). The figure shows that an anti-correlation is seen in both the subsamples of sightlines having Mg II absorbers as well as in subsample of sightlines without any intervening absorbers, with Pearson correlation coefficient, ρ_p , of -0.70 and -0.87 respectively. In [Fig. 8](#), we have also plotted the cumulative probability distribution of fractional polarization for the subsamples with and without Mg II absorbers. We applied K-S test on these two distributions of p which shows that the null hypothesis for them is ruled out at a confidence level of 73%, which is not very significant. The median (mean) value of p for the sample with and without Mg II absorber are found to be 3.70 (4.11) % and 3.92 (4.31) %, respectively. This may indicate again a tentative trend that subsample with Mg II absorbers reduces the fractional polarization in general, but the difference being small have precluded us to make any firm statement on the significant role of intervening absorbers to decrease the p value. On the other hand, the observed strong anti-correlation found for both the subsamples (i.e., with and without Mg II absorbers) indicate the cause of the anti-correlation may be intrinsic to the polarised quasars. This is also consistent with the conclusion drawn by [Farnes et al. \(2014b\)](#), where they have used 599 sources and found that depolarization is predominantly occurring in the local environment of the background quasars.

Additionally, we also checked the effect of the presence of intervening absorbers separately in flat and steep spectrum sources, by comparing their respective CPDFs based on subsamples with and without Mg II absorbers as shown in [Fig. 9](#). For the subsample of flat sources, we found using K-S test, that their CPDF of the sightlines with Mg II absorbers are different from that for the sightlines without Mg II absorbers at 92% confidence level (e.g., see left panel of [Fig. 9](#)). This for steep spectrum source is found to be at 12% confidence level (e.g., see right panel of [Fig. 9](#)). This implies tentatively that there exist effects of Mg II absorbers on the p value for the flat-spectrum sources (i.e., core dominated) having more depolarisation for sightline with Mg II absorbers. However, such an effect is absent in the steep spectrum sources, having more extended radio-emitting regions. This hints at a nominal contribution of these intervening absorbers towards depolarisation. However, the dominant contribution towards depolarization seems to be due to the

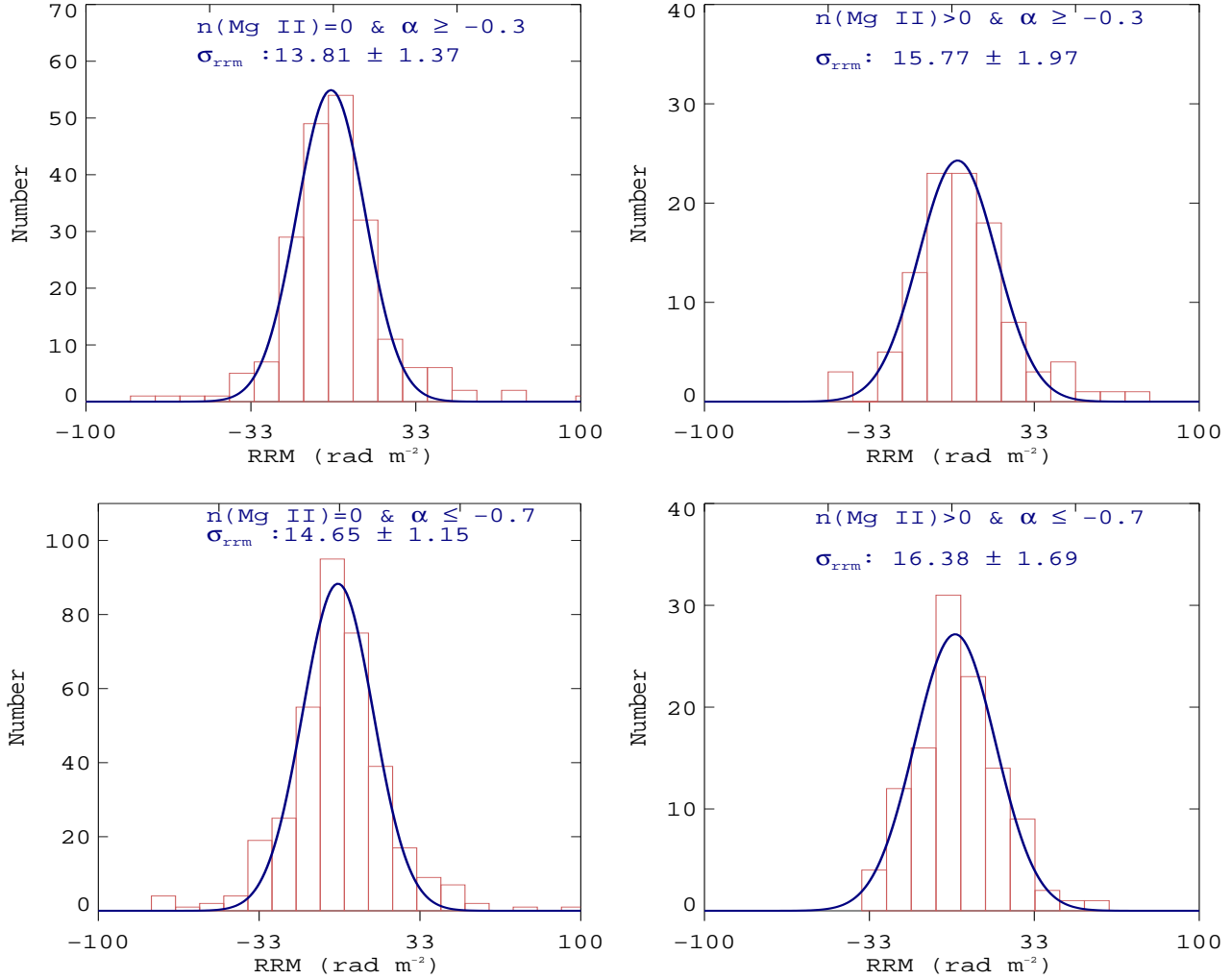


FIG. 5.— Histogram of RRM (red solid line) for sample of our source with radio spectral slope, $\alpha \geq -0.3$ (upper two panels) and $\alpha \leq -0.7$ (lower two panels) splitted in subsamples of sightlines without Mg II absorbers (left column) and with Mg II absorbers (right column). The value of width of Gaussian fit (shown in blue solid line) along with its error bar based on Monte-Carlo simulation are also given.

TABLE 5
RESULTS OF RRM DISTRIBUTION FOR VARIOUS SUBSAMPLE SPLITTED BASED ON RADIO SPECTRAL INDICES ($F_\nu \propto \nu^\alpha$) AND NUMBER OF ABSORBERS.

Sample type	Quasars with $n(\text{Mg II}) = 0$		Quasars with $n(\text{Mg II}) > 0$		Excess ^a
	Sources	$\sigma_{rrm} \pm \delta\sigma_{rrm}$	Sources	$\sigma_{rrm} \pm \delta\sigma_{rrm}$	
$\alpha \geq -0.3^b$	209	13.81 ± 1.37	103	15.77 ± 1.97	7.59 ± 4.78
$\alpha \leq -0.7^c$	356	14.65 ± 1.15	113	16.38 ± 1.69	7.70 ± 4.43

^aExcess for subsample of $n(\text{Mg II}) > 0$ is computed with respect to the $n(\text{Mg II}) = 0$ subsample (e.g., see Eqs. 4 and 5).

^bFlat spectrum radio quasars.

^cSteep spectrum radio quasars.

local environment of the background quasar as revealed by the strong anti-correlation of σ_{rrm} versus p (e.g., see lower panel of Fig. 7) found for both with and without Mg II absorbers subsamples.

4.4. The redshift evolution of RRM and fractional polarisation

Any trend with redshift in the dispersion of RRM and value of polarisation could be a useful tracer of the evolution of cosmic magnetic fields. To study any redshift

dependence of σ_{rrm} and p , we have first compared the CPDFs of emission redshift of subsamples with Mg II absorbers to the subsamples without such absorbers, as shown in the top panel of Fig. 10. Indeed, the fraction of sightlines having a larger number of Mg II absorbers corresponds to sources with higher emission redshift, as is clear from the figure. This is not surprising because farther the sources, higher will be the probability of the sightline passing through more number of intervening absorbers as well as larger the column density of IGM

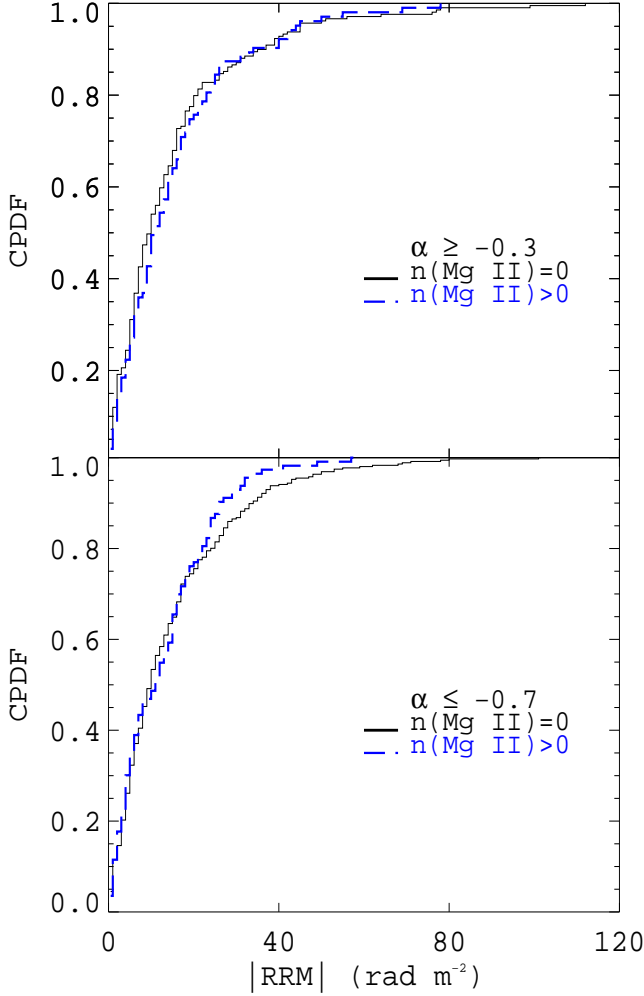


FIG. 6.— *Top panel:* The CPDF of the absolute value of RRM (i.e., $|RRM|$), for the flat spectrum quasar with $\alpha \geq -0.3$ (312 sources) for their subsamples without (black solid line) and with Mg II absorbers (blue dashed line). *Bottom panel:* same as top, but for the $\alpha \leq -0.7$ subsample (469 sources).

through which the sightline has passed. In order to estimate the contribution of Mg II systems, we first need to check the contribution of the IGM.

For this, we have plotted the standard deviation of RRM in different z_{emi} bin in the middle panel of Fig. 10, separately for the subsample with and without Mg II absorbers. As can be seen from this figure, the RRM dispersion of the subsample without Mg II absorbers does not show any significant evolution with z_{emi} over the range of 0.5 to 2.0 as compared to those with Mg II absorbers for the same range in z_{emi} . This indication of negligible evolution (if at all) of RRM with z_{emi} (for sightlines without Mg II systems) suggest that there is probably no significant redshift evolution of the IGM magnetic field to have a noticeable impact on the RRM value and hence can be neglected as compared to the other sources of redshift evolution of σ_{rrm} . This fact also motivates us to compute the σ_{rrm} in different bins of absorber redshift of

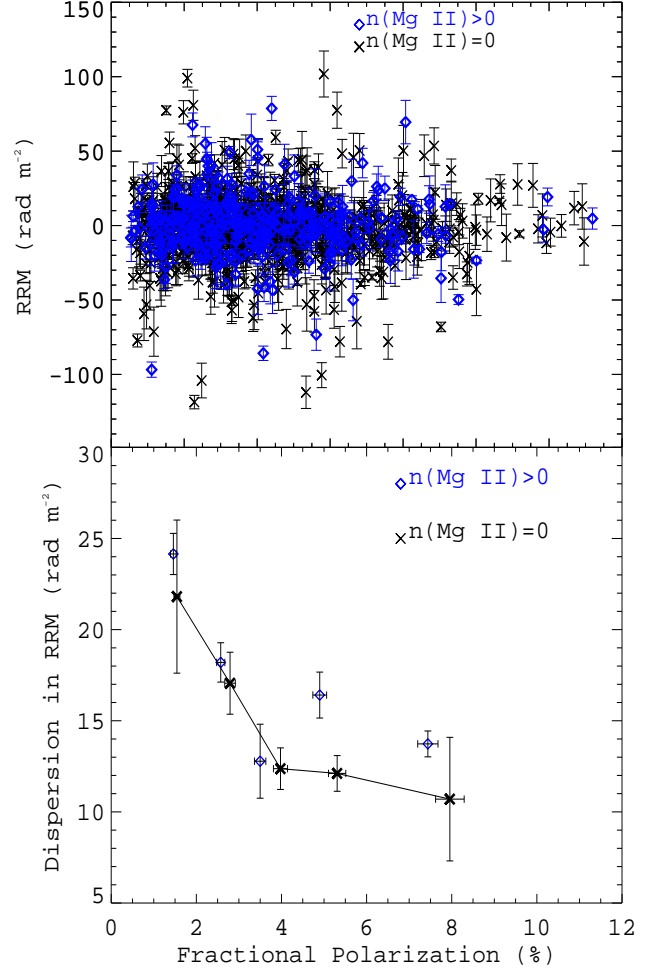


FIG. 7.— *Upper panel:* Distribution of RRM (with 1σ error bar) with the fractional polarization percentage, p , for sources with (blue diamond) and without (black cross) Mg II absorbers along the quasar’s sightline. *Lower panel:* The plot of dispersion in RRM with the fractional polarization for subsamples with (blue diamond) and without (black star) Mg II absorbers.

intervening Mg II absorbers (i.e., z_{abs}) in order to study the contribution of the latter. Any trend in σ_{rrm} versus z_{abs} will be crucial to constrain the magnetic field evolution of these high redshift galaxies (responsible for the Mg II absorbers). For this purpose we plotted σ_{rrm} versus z_{abs} in Fig. 11 using the subsample of 237 sightlines having one Mg II absorber. As can be seen from this figure that there is a clear trend of increasing σ_{rrm} with z_{abs} . Though error bars are large due to the small number of sightlines, the correlation seen between σ_{rrm} versus z_{abs} with ρ_p of 0.85 is very strong. Such a trend will be key to constraint the various model of magnetic field evolution at high redshift galaxies.

Similarly, in the bottom panel of Fig. 10 we also explored the redshift evolution (with z_{emi}) of the median fractional polarisation by using our sample with and without Mg II absorbers. It can be noted from this figure that for the subsample without Mg II absorbers there is almost no evolution of fractional polarisation. However, for the subsample with Mg II absorbers, the fractional

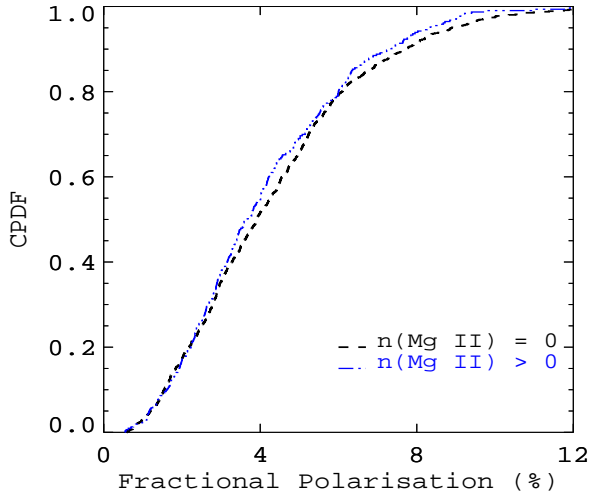


FIG. 8.— The CPDFs of the fractional polarization percentage, p , for subsample with (blue dashed line) and without (black dot-dashed line) Mg II absorbers.

polarisation shows a nominal decreasing trend at higher redshift. This can be reconciled with the fact that the higher redshift bins have more chances to intersect the intervening galaxies (e.g., see top panel of, Fig. 10). This will result in more number of Mg II absorbers per unit redshift path for high redshift quasars, which can lead to the nominal decreasing trend in fractional polarisation that we have seen with the increasing z_{emi} bin.

5. DISCUSSION AND CONCLUSIONS

The Faraday rotation is an important observational tool to estimate the magnetic field and its redshift evolution at high redshift galaxies. For such purposes we addressed the following questions: (i) Does dispersion of RRM distribution correlates with the presence of intervening galaxies searched based on intervening Mg II systems? (ii) Does the sample split based on the radio spectral index, show a difference in the above correlations? (iii) How is the RRM dispersion related to fractional polarisation, and is there any evolution of these observational quantities with the redshift?

In our analysis, we make use of a sample of 1132 quasars, selected by cross-correlating the existing largest catalog of RMs compiled by Taylor et al. (2009) consisting of 37,543 sources and the optical catalogs of Mg II systems by ZM13 using SDSS DR-7, 9 and by RS16 using SDSS DR-12, 14 (e.g., see Sect. 2). We may be noted that our sample is about a factor of two larger as compared to the similar studies by Joshi & Chand (2013) and Farnes et al. (2014b) consisting of 539 and 599 sources respectively. These two studies till now were mainly using the largest sample from the parent sample of RMs at a 21 cm wavelength. The additional sources we could add here are based on new measurements of quasar spectra from SDSS DR-12, 14. Similar study based on 6 cm is carried out by Bernet et al. (2008), though with much smaller sample size of 76 sources (e.g., see Sect. 1).

Our analysis, based on this enlarged sample shows that the RRM distribution width of our sample correlated with the presence of the intervening Mg II sys-

tems with an excess in RRM dispersion of 5.93 ± 2.99 rad m^{-2} (e.g., Sect. 4.1), being higher for the subsample with Mg II systems as compared to the subsample without such Mg II absorption systems. This shows that the intervening galaxies responsible for these intervening Mg II systems do have a contribution in the RRM though at moderate significance of 1.98σ level detected with our enlarged sample. This result is also consistent with the previous similar result by Joshi & Chand (2013), where they also reported an excess of 8.11 ± 4.83 though their confidence level of 1.67σ is mildly smaller than ours (being at 1.98σ level), perhaps due to our larger sample size. It may also be noted that in many previous studies using RRM at 21 cm (e.g., Joshi & Chand 2013; Farnes et al. 2014b) the RRM analysis was based on the measure of dispersion in RRM distribution of subsample with and without Mg II systems. However in our analysis presented here, we have fitted the RRM distribution by a Gaussian function to determine the distribution width (e.g., see Sect. 4.1), which has an additional advantage that such fitting will be less affected by an outlier. We may recall here that the excess RRM contribution due to intervening absorbers exist at RM measurement at 6 cm at even much higher significance (e.g., see Bernet et al. 2008, 2010, 2013; Kim et al. 2016) even with relatively smaller sample (e.g., see Sect. 1). The lower confidence as found in this study (also by, Joshi & Chand 2013) may be due the fact that intervening absorber might also be acting as an inhomogeneous Faraday screen, diluting RRM contribution more at 21 cm compare to at 6 cm as proposed by Bernet et al. (2012).

On the other hand, to test the alternative possibility of frequency-dependent observational selection bias as proposed by Farnes et al. (2014b), we also carry out the analysis of RRM by dividing the parent sample into flat-spectrum and steep-spectrum subsamples (e.g see Sect. 4.2). In our analysis, we did not find any statistically significant difference while comparing the width of RRM distribution between sightlines with and without Mg II absorbers, for both the classes of steep and flat-spectrum sources (e.g., see Sect. 4.2, and Table 5). However, the K-S test reveals that null probability of RRM subsample with and without Mg II absorber, being drawn from the same distribution was higher (52%) for the class of steep spectrum subsample compared to its lower value (15%) for the class of FSRQs. This may be considered as a tentative trend, but we note that our significance level is much smaller than the Farnes et al. (2014b) result, where they found RM verses Mg II system correlation at 3.5σ level for FSRQ compared to no correlation in steep spectrum sources. The possibility of any bias by the RM analysis in the Farnes et al. (2014b) result compared to our RRM based analysis is also ruled out, using a subsample of 462 sources found common between these two studies, for which our analysis agrees with the Farnes et al. (2014b) results. So, it seems likely that for RRM analysis both the factors, frequency-dependence observational selection bias as well as the inhomogeneous Faraday screen diluting the RRM by intervening absorbers, may be at play. Additionally we add here that, since the SDSS spectra do not allow us to search for Mg II systems below the redshift of 0.38, due to lowest spectral coverage limit of 3800 Å in SDSS spec-

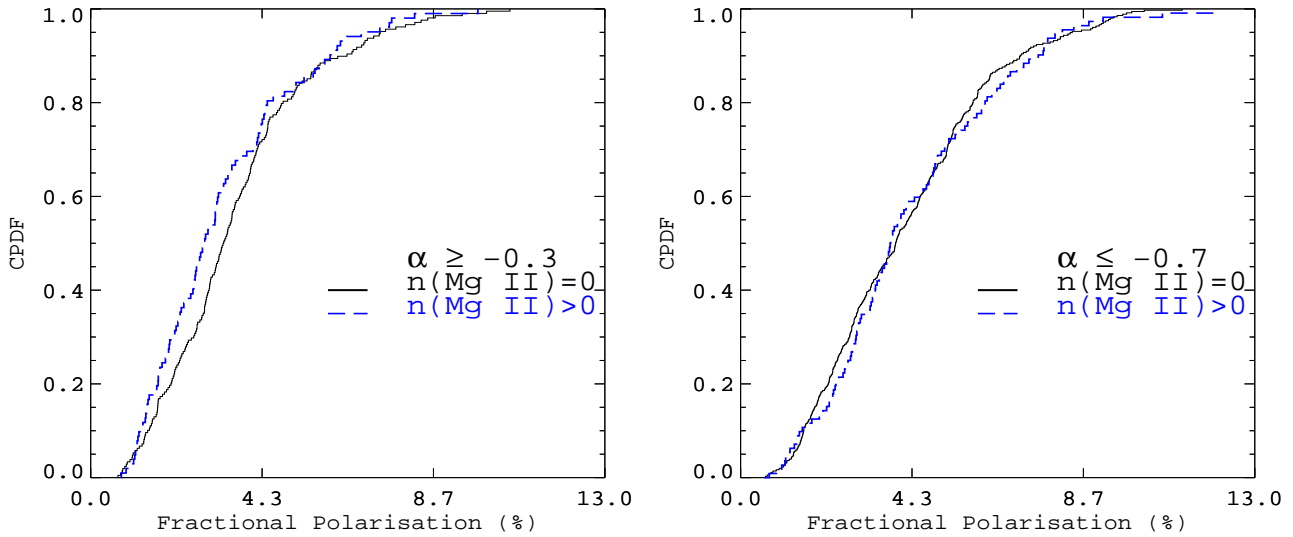


FIG. 9.— *Left panel:* The CPDFs of the fractional polarization percentage, p , for the quasar with no absorber (black thin line), with absorbers (blue dashed line) for $\alpha \geq -0.3$. *Right panel:* same as left, but for quasars sample with $\alpha \leq -0.7$ measurements.

trograph, some of the sightlines without Mg II systems may be contaminated by Mg II system with $z_{abs} < 0.38$, though its effect might not be significant due to our total large redshift range (i.e., $0.38 \leq z_{emi} \leq 2.3$).

Other important additional advantages of our enlarged sample are that we could divide the sample in various bins of redshift and fractional polarisation, and test how the dispersion in RRM evolves with these parameters. In our analysis of RRM we find a very clear anti-correlation among dispersion in RRM versus fractional polarisation, with Pearson correlation coefficient of -0.70 and -0.87 for the subsample with and without Mg II absorbers (e.g., see Sect. 4.3, and Fig. 7). This strong anticorrelation in both with and without Mg II absorbers, in conjunction with the very nominal decrement in the subsample of sightlines with Mg II absorbers clearly shows that the main contribution for the decrement in the fractional polarisation is intrinsic to the environment of the quasars. As can be noted from our plots of RRM dispersion versus the fractional polarisation shown in the lower panel of Fig. 7, the typical difference in σ_{rrm} in all the fractional polarisation bins for subsample with and without Mg II absorber are smaller than 5 rad m^{-2} . This is smaller than the 10 rad m^{-2} value found by Kim et al. (2016), though they use a different technique of rotation measure synthesis over a rather smaller sample size (49 unresolved quasars). On the other hand, the variation in σ_{rrm} (e.g., see Fig. 7) is found to be quite high, typically more than 10 rad m^{-2} over a range of fractional polarisation of about 8%. This suggests that the effect of the intervening absorber is nominal both on the σ_{rrm} and the fractional polarisation (measurement at the 21 cm wavelength), but the strong anti-correlation between these parameters seem to be associated intrinsically to the background source, which might have interesting implication and need further investigations.

The redshift evolution of σ_{rrm} will also be an important check, before interpreting our above strong anti-correlation between RRM dispersion versus fractional

polarisation, due to the available large redshift range of our samples ($0.38 \leq z_{emi} \leq 2.3$). As discussed in Sect. 4.4, for the redshift evolution of intrinsic RRM contribution from background source we have used our 818 sightlines without intervening absorbers, by measuring σ_{rrm} at different z_{emi} bins. As shown in Fig. 10, it is clear that the intrinsic RRM contribution has almost negligible evolution with emission redshift of the background source, and hence may be dominated rather by the local physical environment of the quasars central engine. This means that fractional polarisation which is highly dependent on the σ_{rrm} should also not have any dependence on the z_{emi} , as indeed is found to be the case in our sample (e.g., see bottom panel Fig. 10). The minor trend of decrement in fractional polarisation seen for our sample with Mg II systems as z_{emi} increase may be due to the bias that higher redshift sources have a higher chance to intercept more number of Mg II absorber (e.g., see top panel Fig. 10) and these absorbers can account for such small decrement.

The above results of the negligible redshift evolution of the intrinsic RRM contribution, suggests that if the plot of observed σ_{rrm} versus redshift bins of Mg II absorber shows any such trend then that can be attributed to redshift evolution of σ_{rrm} due to the intervening galaxy at different redshifts. Indeed, by using the sample of background quasars with single absorber, we do see a trend of increasing σ_{rrm} at various bins of z_{abs} , with Pearson correlation coefficient of 0.85 (e.g., see Fig. 11 and Sect. 4.4). This trend will be very useful to infer the redshift evolution of magnetic field strength in the high-redshift galaxies and further demonstrates the importance of the large statistical samples as we have attempted here for such studies.

In summary, our enlarged sample of 1132 sources having both RRM measurements (at 21 cm wavelength) as well as homogeneous optical spectra from SDSS (to separate the sightline with and without Mg II absorber), based on the observations of RRM and fractional polar-

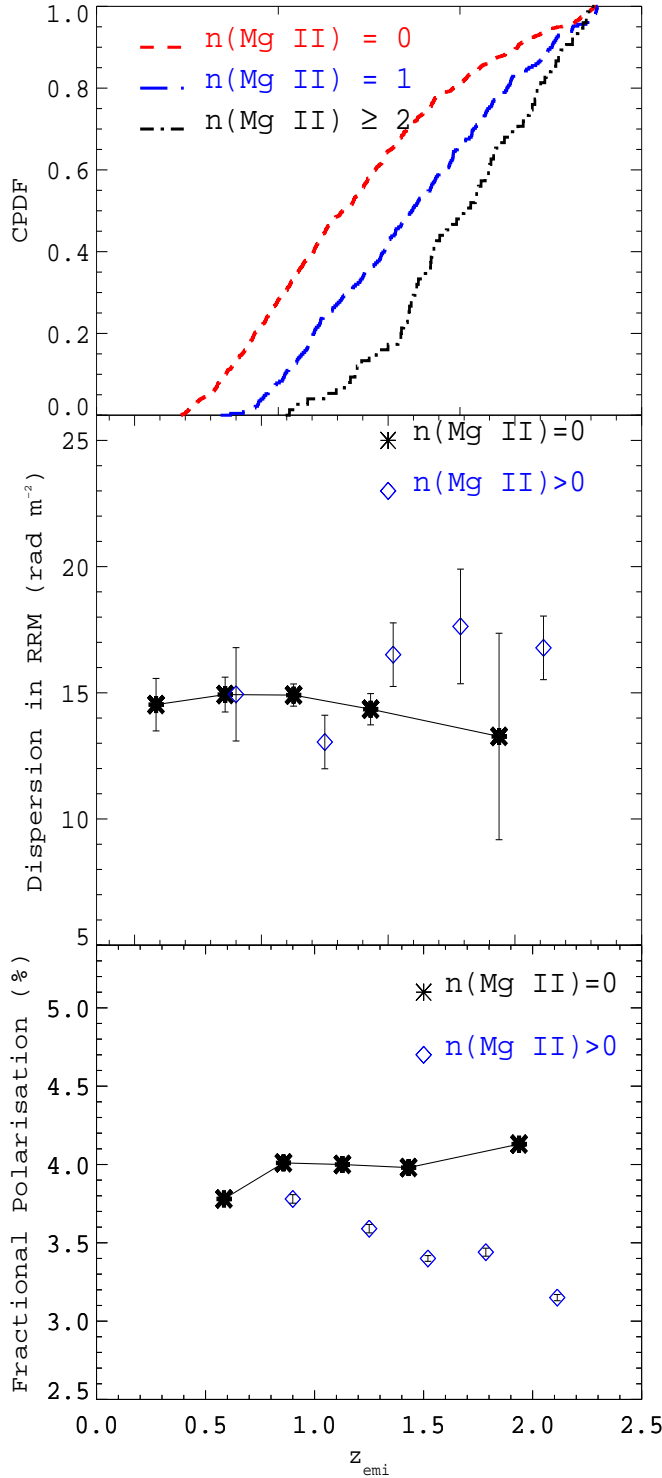


FIG. 10.— Top panel show CPDF for $n(\text{Mg II})=0$ (red dashed line), $n(\text{Mg II})=1$ (blue dashed line) and $n(\text{Mg II})=2$ (black dotted line). The P_{null} of latter two with respect to $n(\text{Mg II})=0$ distribution is 4.49×10^{-09} % and 1.35×10^{-15} % respectively. The middle and lower panel shows respectively the dispersion of RRM and fractional polarisation with emission redshift of the quasar, z_{emi} , for subsample without Mg II absorber (black star), and for with Mg II absorbers (blue diamond).

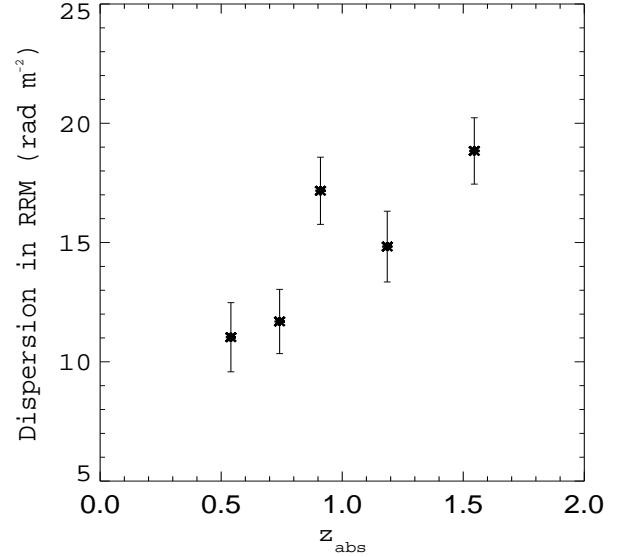


FIG. 11.— Dispersion of the RRM with the absorbers redshift of intervening Mg II absorbers, z_{abs} , for subsample of 237 sources with one intervening Mg II absorbers in their line of sight.

isation has allowed us to draw the following main conclusions regarding the magneto-active plasma at high-redshift galaxies: (i) The RRM distribution width of our sample correlated with the presence of intervening Mg II systems with an excess in RRM dispersion of $5.93 \pm 2.99 \text{ rad m}^{-2}$ (i.e., at 1.98σ level) being higher for the sample with Mg II systems as compared to the sample without such absorption systems. The effect of EW_r of Mg II absorber on σ_{rrm} is found nominal with being higher for higher EW_r . (ii) The subsample split based on the radio spectral index does not show a significant difference in the above correlation. (iii) An anti-correlation is found between the dispersion in RRM and fractional polarisation with a Pearson correlation coefficient of -0.70 and -0.87 for the sample with and without Mg II absorbers, respectively. In this anti-correlation, the impact of the presence of the Mg II absorbers is found to be very nominal (e.g., to increase the σ_{rrm}), suggesting that the contribution for the decrement in the fractional polarisation is mainly intrinsic to the environment of the quasars. This is further supported by the absence of any significant evolution of either σ_{rrm} or of the median value of the fraction polarisation at various z_{emi} bins using the subsample without Mg II absorbers. (iv) A very significant redshift evolution of σ_{rrm} at various z_{abs} bins using the subsample with single Mg II absorption is revealed in our analysis with Pearson correlation of 0.85 , which can be very useful to further constrain the redshift evolution of magnetic field strength of the high-redshift galaxies. Further improvements on these aspects will be possible with the enlargement of the sample having both optical spectra as well as radio polarisation measurements. Surveys, such as the square kilometer array (SKA) as well as future optical data release such as of SDSS can play crucial roles in such studies.

ACKNOWLEDGMENTS

SM, HC and TRS acknowledge the facilities at IRC, University of Delhi. SM and TRS also thank ARIES for the hospitality. TRS and HC acknowledge the project grant from SERB, Govt. of India (EMR/2016/002286). The research of SM is supported by UGC, Govt. of India under the UGC-JRF scheme (Sr.No. 2061651305 Ref.No: 19/06/2016(I) EU-V).

Funding for the SDSS and SDSS-II has been provided by the Alfred P. Sloan Foundation, the Participating Institutions, the National Science Foundation, the U.S. Department of Energy, the National Aeronautics and Space Administration, the Japanese Monbukagakusho, the Max Planck Society, and the Higher Education Funding Council for England. The SDSS Web Site is <http://www.sdss.org/>. The SDSS is managed by the Astrophysical Research Consortium for the Participating Institutions. The Participating Institutions are the American Museum of Natural History, Astrophysical Institute Potsdam, University of Basel, University of Cambridge, Case Western Reserve University, University of Chicago, Drexel University, Fermilab, the Institute for Advanced Study, the Japan Participation Group, Johns Hopkins University, the Joint Institute for Nuclear Astrophysics and Cosmology, the Korean Scientist Group, the Chinese Academy of Sciences (LAMOST), Los Alamos National Laboratory, the Max-Planck-Institute for Astronomy (MPIA), the Max-Planck-Institute for Astrophysics (MPA), New Mexico State University, Ohio State University, University of Pittsburgh, University of Portsmouth, Princeton University, the United States Naval Observatory, and the University of Washington.

REFERENCES

- Basu, A., Mao, S. A., Fletcher, A., et al. 2018, *MNRAS*, **477**, 2528
 Bergeron, J., & Stasińska, G. 1986, *A&A*, **169**, 1
 Bernet, M. L., Miniati, F., & Lilly, S. J. 2010, *ApJ*, **711**, 380
 Bernet, M. L., Miniati, F., & Lilly, S. J. 2012, *ApJ*, **761**, 144
 Bernet, M. L., Miniati, F., & Lilly, S. J. 2013, *ApJ*, **772**, L28
 Bernet, M. L., Miniati, F., Lilly, S. J., Kronberg, P. P., & Dessauges-Zavadsky, M. 2008, *Nature*, **454**, 302
 Bhat, P., & Subramanian, K. 2013, *MNRAS*, **429**, 2469
 Chen, H.-W., & Tinker, J. L. 2008, *ApJ*, **687**, 745
 Churchill, C. W., Kacprzak, G. G., & Steidel, C. C. 2005, in *IAU Colloq. 199: Probing Galaxies through Quasar Absorption Lines*, ed. P. Williams, C.-G. Shu, & B. Menard, 24
 Farnes, J. S., Gaensler, B. M., & Carretti, E. 2014a, *ApJS*, **212**, 15
 Farnes, J. S., O'Sullivan, S. P., Corrigan, M. E., & Gaensler, B. M. 2014b, *ApJ*, **795**, 63
 Hammond, A. M., Robishaw, T., & Gaensler, B. M. 2012, arXiv:1209.1438, [arXiv:1209.1438](https://arxiv.org/abs/1209.1438) [[astro-ph.CO](https://arxiv.org/abs/1209.1438)]
 Han, J. L., Manchester, R. N., Lyne, A. G., Qiao, G. J., & van Straten, W. 2006, *ApJ*, **642**, 868
 Joshi, R., & Chand, H. 2013, *MNRAS*, **434**, 3566
 Kacprzak, G. G., Churchill, C. W., Steidel, C. C., & Murphy, M. T. 2008, *AJ*, **135**, 922
 Kim, K. S., Lilly, S. J., Miniati, F., et al. 2016, *ApJ*, **829**, 133
 Kronberg, P. P., Bernet, M. L., Miniati, F., et al. 2008, *ApJ*, **676**, 70
 Kronberg, P. P., & Perry, J. J. 1982, *ApJ*, **263**, 518
 Kronberg, P. P., Reinhardt, M., & Simard-Normandin, M. 1977, *A&A*, **61**, 771
 Kronberg, P. P., & Simard-Normandin, M. 1976, *Nature*, **263**, 653
 Mao, S. A., Carilli, C., Gaensler, B. M., et al. 2017, *Nature Astronomy*, **1**, 621
 Mestel, L., & Paris, R. B. 1984, *A&A*, **136**, 98
 Narayanan, A., Misawa, T., Charlton, J. C., & Kim, T.-S. 2007, *ApJ*, **660**, 1093
 Neronov, A., Semikoz, D., & Banafsheh, M. 2013, arXiv e-prints, arXiv:1305.1450
 Oren, A. L., & Wolfe, A. M. 1995, *ApJ*, **445**, 624
 Raghunathan, S., Clowes, R. G., Campusano, L. E., et al. 2016, *MNRAS*, **463**, 2640
 Rees, M. J. 1987, *QJRAS*, **28**, 197
 Roy, S., Pramesh Rao, A., & Subrahmanyam, R. 2008, *A&A*, **478**, 435
 Schnitzeler, D. H. F. M. 2010, *MNRAS*, **409**, L99
 Short, M. B., Higdon, D. M., & Kronberg, P. P. 2007, *Bayesian Analysis*, **2**
 Steidel, C. C. 1995, in *QSO Absorption Lines*, ed. G. Meylan, 139
 Stil, J. M., Taylor, A. R., & Sunstrum, C. 2011, *ApJ*, **726**, 4
 Taylor, A. R., Stil, J. M., & Sunstrum, C. 2009, *ApJ*, **702**, 1230
 Vacca, V., Murgia, M., Govoni, F., et al. 2018, *Galaxies*, **6**, 142
 Watson, A. M., & Perry, J. J. 1991, *MNRAS*, **248**, 58
 Welter, G. L., Perry, J. J., & Kronberg, P. P. 1984, *ApJ*, **279**, 19
 Xu, J., & Han, J.-L. 2014a, *Research in Astronomy and Astrophysics*, **14**, 942
 Xu, J., & Han, J. L. 2014b, *MNRAS*, **442**, 3329
 You, X. P., Han, J. L., & Chen, Y. 2003, *Acta Astronomica Sinica*, **44**, 155
 Zhu, G., & Ménard, B. 2013, *ApJ*, **770**, 130
 Zibetti, S., Ménard, B., Nestor, D. B., et al. 2007, *ApJ*, **658**, 161